2010

Friction stir processing (FSP) of cast metals: microstructure-property relationships in NiAl bronze and AA5083

McNelley, T.R.; Swaminathan, S.; Menon, S.K.; Su, J.-Q.

TransTech Publications

T.R. McNelley, S. Swaminathan, S.K. Menon, J.-Q. Su, "Friction stir processing (FSP) of cast metals: Microstructure-property relationships in NiAl bronze and AA5083," Materials Science Forum, (2010), v. 638-642, pp. 35-40.

http://hdl.handle.net/10945/55372

Materials Science Forum *Online: 2010-01-12*
ISSN: 1662-9752, Vols. 638-642, pp 35-40
doi:10.4028/www.scientific.net/MSF.638-642.35

Friction Stir Processing (FSP) of Cast Metals: Microstructure – Property Relationships in NiAl Bronze and AA5083

T.R. McNelley[1,a], S. Swaminathan[2,b], S.K. Menon[1,c] and J.-Q. Su[1,d]

[1]Department of Mechanical and Astronautical Engineering, Naval Postgraduate School, Monterey, CA 93943-5146 USA

[2]GE Global Research, Export Promotion Industrial Park, Bangalore, Karnataka, 560066 INDIA

[a]tmcnelley@nps.edu, [b]srinivasan.swaminathan@ge.com, [c]skmeno1@nps.edu, [d]jsu@nps.edu

Keywords: Friction stir processing; Multi-pass processing; Microstructure control; Temperature distribution; Strain distribution; Mechanical properties; Superplasticity.

Abstract. Parameters for multi-pass FSP include the pattern of tool traverse and step-over distance between successive passes. Multi-pass FSP was conducted on as-cast NiAl bronze and as-cast AA5083 in order to modify stir zone (SZ) microstructures and mechanical properties. Highly refined and homogeneous SZ microstructures may be produced by FSP. Refined and equiaxed grain structures reflect recrystallization during FSP; mechanisms leading to homogenization by redistribution of microstructure constituents remain to be determined. Refined microstructures exhibit enhanced ambient-temperature properties and superplasticity at elevated temperatures.

Introduction

FSP is an allied process of friction stir welding (FSW) [1] and may be employed to achieve localized modification of microstructures in the surface layers of deformable cast or wrought metals. In FSP, a cylindrical, wear-resistant tool consisting of a smaller diameter pin with a concentric, larger diameter shoulder is rotated and forced into a surface of the work piece, as illustrated in Fig. 1a. As the tool pin penetrates, a combination of frictional and adiabatic heating softens the material so that tool rotation induces a stirring action and flow of material about the pin from the advancing side to the retreating side of the tool. Severe but localized plastic deformation results in formation of the SZ while adjacent regions experience only moderate straining and comprise the thermomechanically affected zone (TMAZ). The tool shoulder prevents upward flow of material and serves to forge the SZ as it comes in contact with the work piece surface; large areas may then be processed by traversing the tool in a pattern on the work piece surface [1-5].

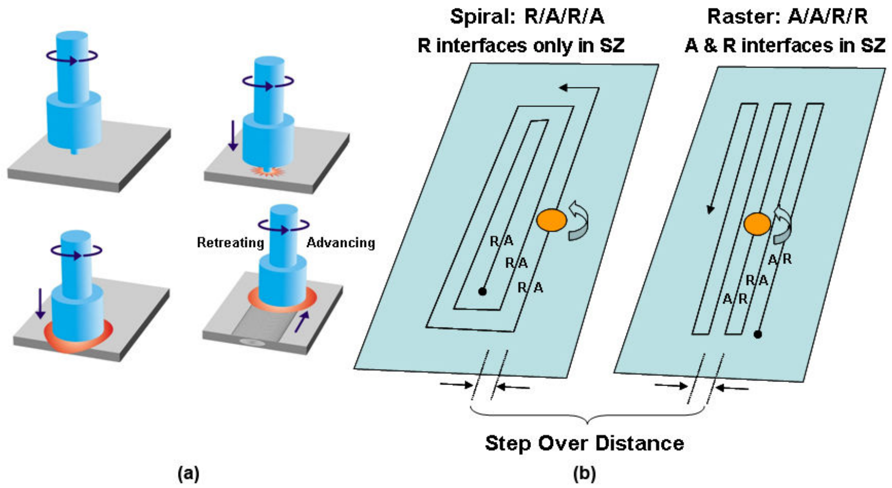

Figure 1. A schematic of FSP [1] is shown in (a); spiral and raster patterns for FSP are illustrated in the schematics in (b), which show that spiral patterns may leave only retreating interfaces (except on the first pass) while raster patterns leave both advancing and retreating interfaces in the SZ.

Traversing patterns in FSP have included repeated linear traverses that are offset from one another by a characteristic step-over distance. Rectangular or circular spiral patterns and raster patterns (see Fig. 1b) have also been employed wherein successive traverses are, again, offset by a characteristic step over distance. Spiral patterns may leave only retreating (or advancing) side interfaces within the SZ while rasters may leave an alternating pattern of advancing and retreating interfaces. When FSP is conducted on as-cast metals, microstructures may be converted to a wrought condition in the absence of macroscopic shape change. Further details of tool design and use, control, and material response to the thermomechanical cycles in FSW/P have been given elsewhere [6].

FSP of NiAl Bronze

Microstructure Refinement. Table 1 gives composition data for NiAl bronze and the alloy of this investigation. Details of the alloy constitution of as-cast material as well as the effect of FSP on microstructure have been given previously [7-10]. Plates, each approximately 300mm × 152mm × 42mm in thickness, were sectioned from a large casting. FSP was conducted using a tool fabricated in Densimet® and having a pin in the shape of a truncated cone 12.7mm in length, a base diameter

Table 1.Compositions (in wt. pct.) of the NiAl bronze alloy in this investigation

Element	Cu	Al	Ni	Fe	Mn	Si	Pb
Min-max	(min)79.0	8.5-9.5	4.0-5.0	3.5-4.5	0.8-1.5	0.10(max)	0.03(max)
Nominal	81	9	5	4	1	-	-
Alloy	81.2	9.39	4.29	3.67	1.20	0.05	<0.005

of 15mm, and tip diameter of 6.3mm. The pin also had a step-spiral thread feature. Various tool rotation and traversing rate combinations were employed. Fig. 2a shows a montage of micrographs from the center of the SZ in material processed at 1200rpm and 51mm min. The tool pin profile is indicated for the first two passes in a spiral pattern (see the inset at left). A uniformly refined SZ microstructure is apparent for a step-over distance of 4.5mm. The base metal microstructure of this alloy is shown in Fig. 2b to consist of the terminal α (fcc) solid solution containing a fine dispersion

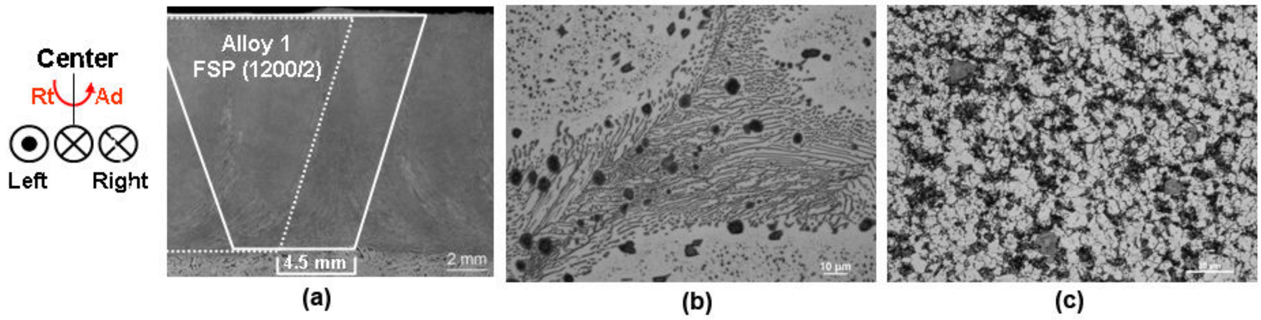

Figure 2. A montage of images of the stir zone with the pin profile superimposed is shown in (a); the base metal microstructure is shown in (b) while the refined and homogeneous stir zone microstructure is shown in (c).

of κ_{iv} (Fe_3Al) particles and a eutectoid decomposition product of the high-temperature β (bcc) phase.comprising α and a lamellar κ_{iii} (NiAl) phase. Coarse κ_{ii} (Fe_3Al) particles are also apparent mainly in the eutectoid product. During mulit-pass FSP, such a microstructure is heated and severely deformed at temperatures of 900 – 1000°C resulting in refinement and homogenization of the resulting microstructure. Such a SZ microstructure is shown in Fig. 2c. The α grains are ~10µm in size. Reversion of the eutectoid, deformation and subsequent transformation at the relatively high cooling rates after FSP result in the formation of fine and dispersed transformation products

Mechanical Properties Benefits of FSP. The highly refined SZ microstructures exhibit increased strength and ductility. Fig. 3a shows a plate of this alloy processed at 800rpm and 102mm min^{-1} before and after sectioning of mechanical test samples by wire EDM. Four different series of tensile samples were prepared: the L2 and T2 series (L: tensile axis is parallel, or T, transverse to the local axis of tool traversing) are from the mid-region of the pattern while L1 and T1 are from the last (outer) pass. Blanks were cut for each sample series and then sliced so that the distance below the plate surface could be ascertained for each individual tensile sample; the blanks were sliced to enable determination of properties from the top of the SZ downward and into base metal. After light grinding to remove machining damage these samples were pulled in tension to failure at a nominal

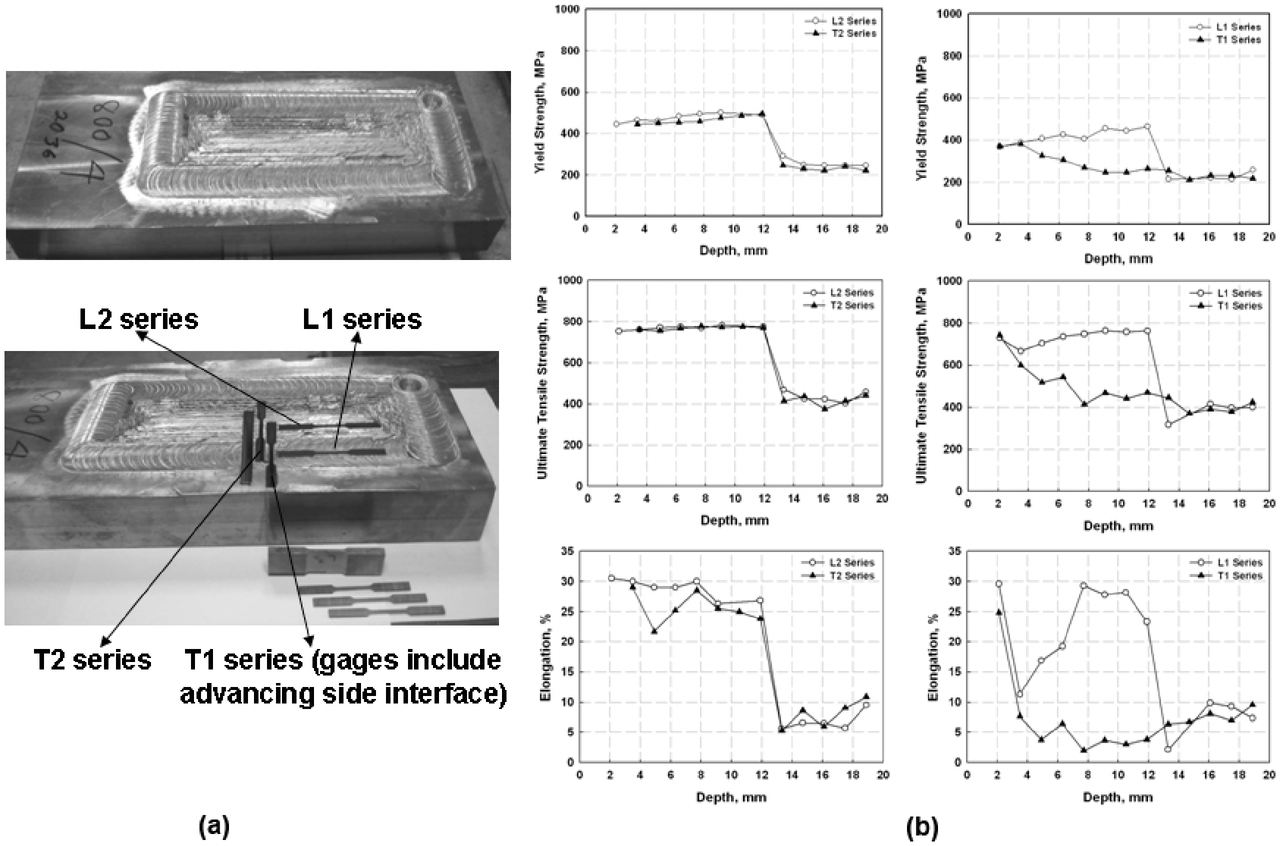

Figure 3. An as-cast plate of NiAl bronze following FSP is shown in (a); tensile test samples were sectioned by wire EDM and tensile properties were determined as a function of depth in the stir zone, as shown in (b)

strain rate of $10^{-3}s^{-1}$. Plots of yield and ultimate strength as well as ductility are shown in Fig. 3b. The L2 and T2 series show that the yield and ultimate strengths both increase from the top surface downward to the bottom of the SZ and then decrease into base metal. Both measures of strength are about 2× their respective values in base metal. Nevertheless, SZ ductility is also improved, indeed by an even larger factor of 3×. A region of reduced ductility immediately below the SZ in the TMAZ reflects mainly a heat effect (a similar effect is present after fusion welding).

The depth dependence of properties in the L1 series is similar to that in the L2 series. However, the transverse properties, i.e., the T1 series, exhibit a pronounced drop in strength and ductility below the plate surface. The samples in question have both stir zone and base metal within their deforming gage sections and the reduced ductility reflects strain localization in the weaker base metal portions of these gage sections. Thus, the potential for reduced properties below and at the periphery of the SZ must be taken into account in applications of FSP.

FSP of As-Cast AA5083

Microstructure Refinement and Homogenization. The composition of the 15mm thick continuously cast AA5083 plate of this investigation is given in Table 2. Five parallel FSP traverses were conducted with a step-over of 2.0mm on a portion of the as-cast plate as shown in Fig. 4a. The tool was fabricated in H13 steel with a 6.2mm long threaded pin having a base diameter of 6.5mm and a tip diameter of 3.5mm. A section through the SZ is shown in Fig. 4b and includes the

Table 2. Compositions (in wt. pct.) of AA5083 alloy in this investigation

Element	Mg	Mn	Si	Fe	Cr	Cu	Al
Min-max	4.0-4.9	0.4-1.0	0.4(max)	0.4(max)	0.05-0.25	0.15(max)	Bal.
Nominal	4.4	0.7	-	-	0.15	-	Bal.
Alloy	4.70	0.72	0.07	0.22	-	0.02	Bal.

approximate gage cross sections of three tensile samples sectioned from the top to the bottom of the stir zone. Optical microscopy images from the as-cast base metal and the SZ are shown in Fig. 5a and b, respectively. The coarse Al_6Mn and Al(Fe,Si) phases present in the as-cast material have been refined and re-distributed in the SZ; nevertheless, there is no apparent damage to either the particles or the matrix after FSP. The extent of SZ grain refinement is apparent in the OIM grain

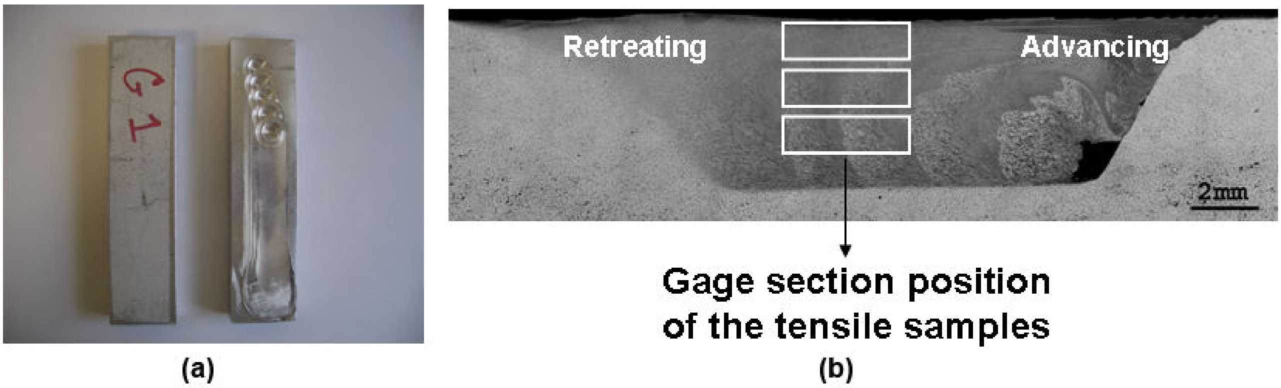

Figure 4. Five FSP traverses were conducted on as-cast AA5083 material as shown in (a); a transverse view of the resulting stir zone is depicted in (b). A tunnel defect is apparent at lower right.

map in Fig. 6a, wherein the mean lineal intercept grain size was determined to be 1.2μm. The corresponding microtexture and grain boundary data in Fig. 6b and c, respectively, indicate that the multi-pass FSP has produced a random texture and misorientation distribution in the SZ. A low-angle peak (at 0 – 5°) likely reflects residual deformation after the last pass of the tool.

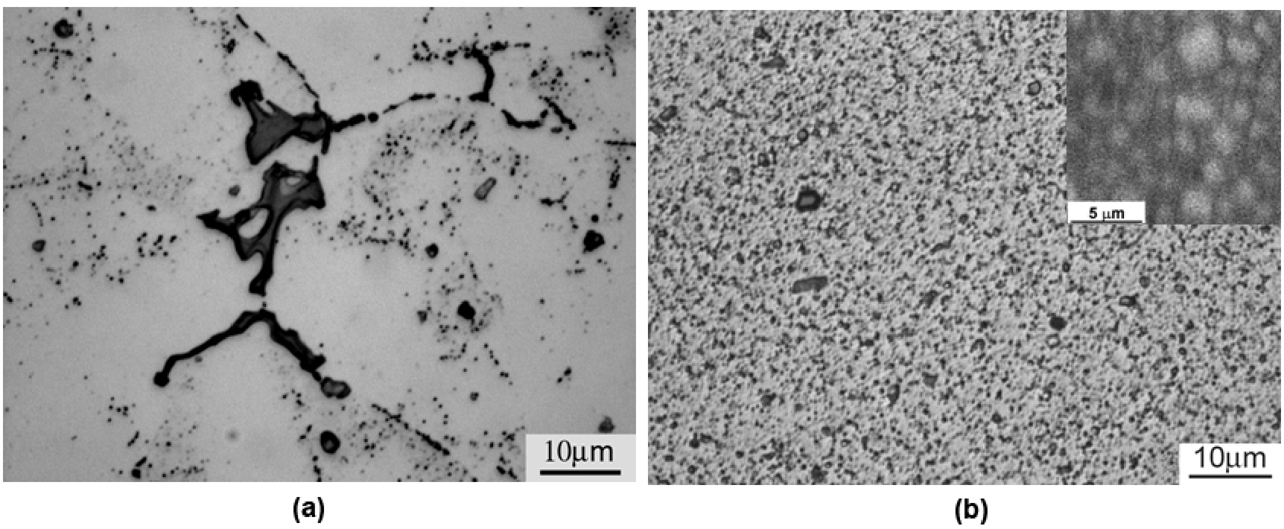

Figure 5. The as-cast AA5083 material is shown in (a) while the stir zone is illustrated in (b). Note the homogenization of microstructure in the absence of damage to the constituents or matrix.

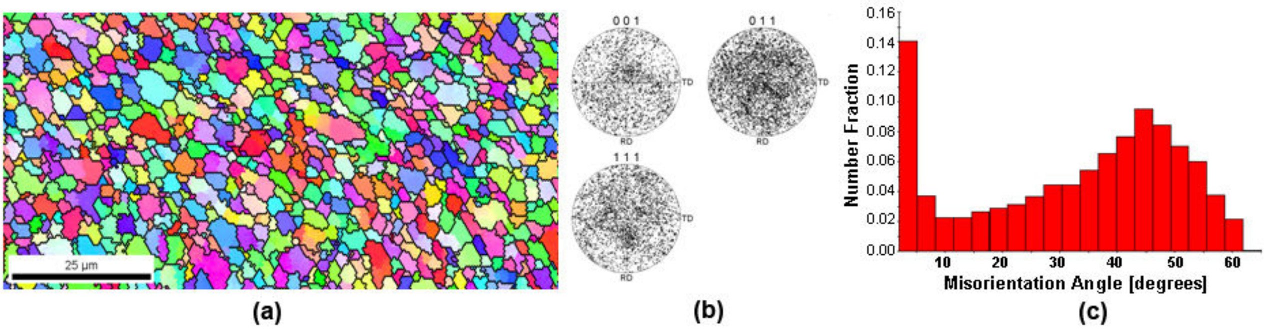

Figure 6. An OIM grain map in (a) demonstrates refinement of the stir zone to grains ~1.2μm in size; a near random texture and misorientation distribution in (b) and (c), respectively, are consistent with recrystallization while a low-angle peak in the misorientation distribution is consistent with residual deformation due to the tool shoulder.

Superplasticity by FSP. Tensile samples having gage lengths of 8mm, widths of 2mm and thickness of 1mm were sectioned by wire EDM. After light grinding to remove machining damage these samples were deformed in tension after equilibration for 20mins in a furnace at 450°C. Test results for a series of five tests on the FS'ed material are compared in Fig. 7 to tests of conventional AA5083 produced by direct-chill casting and hot and cold rolling to 1.4mm thickness, and continuously cast AA5083 after conventional hot and cold rolling to the same thickness [11-14]. FSP has resulted in a reduction in flow stress and increase in strain rate for the maximum value of the strain rate sensitivity coefficient, $m \equiv \partial \ln \sigma / \partial \ln \dot{\varepsilon}$. Indeed, $m \cong 0.5$ at a strain rate $\dot{\varepsilon} = 10^{-1}\,\mathrm{s}^{-1}$ for FS'ed material while the conventionally processed materials only exhibit such an *m* value at strain rates two orders of magnitude lower than this. The ductility versus strain rate data illustrate the enhanced superplastic ductility of the FS'ed material. A maximum elongation >1200pct. was

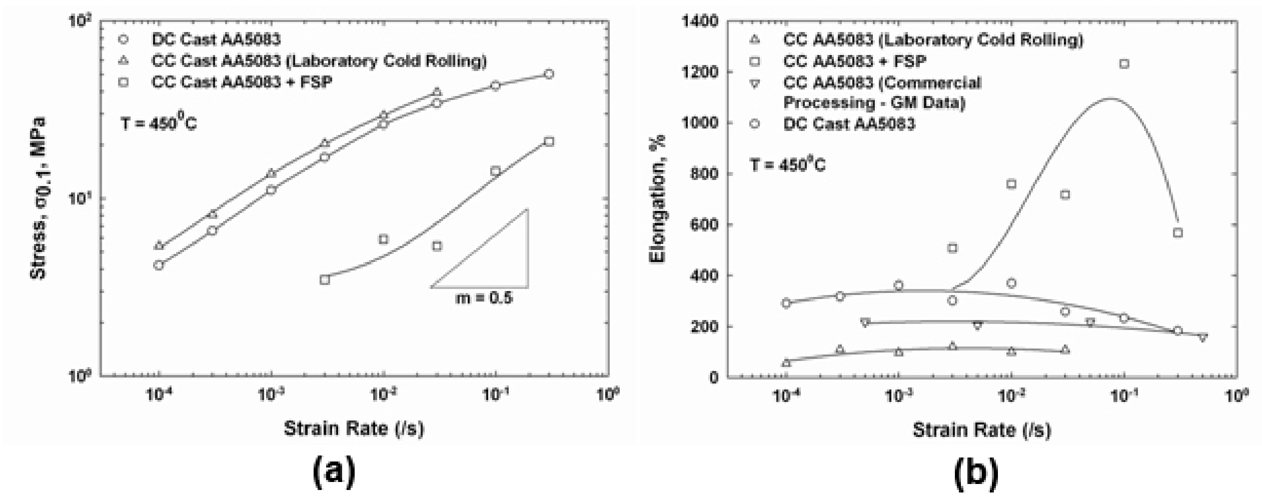

Figure 7. Plots of flow stress (at a strain of 0.1) as a function of strain rate are shown in the graph in (a) for conventionally processed AA5083 materials and the as-cast and FSP'd AA5083; the stir processed material deforms at lower stresses and higher strain rates. The peak ductility for the stir processed material corresponds to the peak m-value of 0.5. The high ductility after processing likely also reflects reduced cavitation.

attained at a strain rate of $10^{-1}\ \mathrm{s}^{-1}$, and this corresponds to the maximum *m* value in the stress versus strain rate data. In contrast, the conventional materials exhibit ductility maxima of 400pct. or less and at strain rates of $10^{-3} - 10^{-2}\ \mathrm{s}^{-1}$.

Summary

FSP enables the conversion of as-cast microstructures to a wrought condition in SZ's. The refinement and homogenization of microstructures in NiAl bronze provide significant improvements in material properties and FSP may be viewed as a means for surface hardening of this material. The application of FSP to as-cast AA5083 material also refines and homogenizes microstructure and results in exceptional superplastic response in this material. In both the NiAl bronze and AA5083 FSP not only refines but also homogenizes microstructures by the re-distribution of constituent particles. The mechanisms of this re-distribution during FSP remain to be clarified.

References

[1] W.M. Thomas, E.D. Nicholas, J.C. Needham, M.G. Murch, P. Templesmith and C.J. Daws: G.B. Patent Application No. 9125978.8, December, 1991; U.S. Patent No. 5460317, October, 1995

[2] R.S. Mishra: *Advanced Materials and Processes*, 2003, vol. 161(10), pp. 43-46

[3] R.S. Mishra, Z.Y. Ma and I. Charit: *Mater. Sci. Engng. A*, 2003, vol. A341, pp. 307-10

[4] Z.Y. Ma, R.S. Mishra and M. W. Mahoney: in *Friction Stir Welding and Processing II*, K.V. Jata, M.W. Mahoney, R.S. Mishra, S.L. Semiatin and T. Lienert, eds., TMS, Warrendale, PA, 2003, pp. 221-30

[5] R.S. Mishra, M.W. Mahoney, S.X. McFadden, N.A. Mara and A.K. Mukherjee: *Scripta Mater.*, 2000, vol. 42, pp. 163-68

[6] TR McNelley, K Oh-Ishi, AP Zhilyaev: "Microstructures and Properties of Copper Alloys after Friction Stir Welding/Processing", Chapter 8 in Friction Stir Welding and Processing (R Mishra and MW Mahoney, eds.), pp. 155 – 73, ASM International, Materials Park, OH, 2007

[7] K Oh-Ishi and TR McNelley: *Metall.Mater. Trans A*, Vol. 36A (2005), pp. 1575 – 85

[8] K Oh-Ishi, AP Zhilyaev and TR McNelley: *Metall Mater Trans A*, Vol. 37A (2006), pp. 2239 – 5

[9] MD Fuller, S Swaminathan, AP Zhilyaev and TR McNelley: *Mater. Sci.Engr A*, Vol. 463 (1-2) (2007), pp. 128 – 37

[10] TR McNelley, S Swaminthan, JQ Su and S Menon: "Microstructure – Processing Relationships in Friction Stir Processing (FSP) of NiAl Bronze", in Friction Stir Welding and Processing V (RS Mishra, MW Mahoney and TJ Lienert, eds.), pp. 3 – 10, TMS, Warrendale, PA, 2009

[11]M.A. Kulas, W.P. Green, E.M. Taleff, P.E. Krajewski and T.R. McNelley: *Metall. Trans. A*, 2005, vol. 36A, pp. 1249 – 61

[12] E.M. Taleff, W.P. Green, M.A. Kulas, T.R. McNelley and P.E. Krajewski: *Mater. Sci Engng. A*, 2005, vol. 410-11, pp. 32 – 7

[13]W.P. Green, M.A. Kulas, A. Niazi, K. Oh-ishi, E.M. Taleff, P.E. Krajewski and T.R. McNelley: *Metall. Mater. Trans A*, 2006, vol. 37A, pp. 2727 – 38

[14] TR McNelley, K. Oh-Ishi, A.P. Zhilyaev, S. Swaminathan. P.E. Krajewski and E.M. Taleff: *Metall. Mater.Trans.A*, Vol. 39A (2008), pp. 50-64